

Research report GAČR nr. 13-20031S 2014

Authors: D. Jašíková, M. Kotek, S. Fialová, F. Pochylý, M. Klíma, V. Kopecký

Keywords: dynamic contact angle, hydrophobic surfaces, impinging droplet method, inclined surface method, shadowgraphy

Abstract – 2nd year of the solution

The aims:

Construction of an experimental device. Testing the experimental device and implementation of a series of experiments using the optical methods, including micro PIV and tomography.

A. Measurement of the fluid slip near hydrophobic surfaces.

B. Measurement of the air layer in the liquid boundary layer near the hydrophobic surface.

C. Evaluation of measurement, correlation with the mathematical model and computational modeling.

A. Measurement of the fluid slip near hydrophobic surfaces.

Introduction

The biggest challenge for humanity is to reduce energy consumption and increase environmental cleanliness. At present the 25% of total produced energy is consumed for pumping liquids. One of the ways to increase global energy saving in this area is the treatment of hydraulic surfaces with hydrophobic layers. The effect of hydraulic machines can be increased by up to 5% and this value represents a significant savings on the national and global scale. The upgrade of pipeline treatment technology could put these savings even higher. [1]

The application of the hydrophobic surfaces in the pipe system and hydraulic machines can significantly reduce shear stress and friction loss. [2]



The hydrophobicity means that the surface resists to the liquid ingress. It is used as self-cleaning glazing of cars and buildings or to increase the life of paints. The novel industrial application can be found in heat exchangers, building construction and water treatment industry. [3]

In nature the hydrophobicity is well known for some species of spiders and plants. The smart surfaces produced by the living organisms are very often caused by the hydrophobicity of the surface covered with small hairs (spiders, plants, Lady's Mantle, Salvinia) or in some plant covered with wax crystals (Lotus leaf, Dicentra). These both covers lead to increase of surface area and organized surface roughness to ensure the development of air layer. This natural-evolution process is also repeated in industrial production of hydrophobic surfaces with highly defined rough structure.

The second way to decrease the hydraulic loses in the flow is the decreasing surface roughness to super smooth surfaces covered with the thin layer of active substance (wax).

Both mentioned techniques are very expensive in development as in production so there is strong demand for the easy to manufacture treating highly mechanical resistant without the negative effect on the degradation of substrate material.

The degree of hydrophobicity is commonly expresses by so-called contact angle (CA) θ of water, which is the angle between the surfaces of defined-volume drop and the contact material. Hydrophobic refers to those materials where the contact angle is greater than 90° . Ultrahydrophobic are such surfaces on which the water contact angle θ is greater than 150° . In the literature there is sometimes confusion between the terms ultrahydrofobicity and superhydrofobicity, when they are taken as synonyms, but the term properly refers superhydrofobic property of the surface material, if the water contact angle θ is in the range of 130° - 150° .

Other important information characterizing the surface properties of the material are the inclination angle or the sliding angle (SA) at which the drop slides along the surface. The last quantifying value is the contact angle hysteresis (CAH) that is manifested when the volume of drops is changing, this value is supposed to be very small for ultrahydrophobic materials. [4]

The interaction between the liquid and the surfaces is described with boundary slip effect that is affected by wall sheer-stress (WSS). With the smart surface problematic comes up the novel boundary condition for the simulation software that has to be set if we use this surface in mathematical models. They're supposed to be dependence between the CA, SA, CAH and the liquid flow behavior close to the wall. [5] This complex close to wall flow field that is based on the momentum and energy interaction with the surface is a difficult issue for description, especially for understanding the basic mechanism.[6-10]

The measurement of the WSS is mostly based on contact and disruptive methods such as hot-film sensor hot-wire anemometry or Preston tube. [11-16] As we were most interested in the direct qualitative description of the flow interaction with the treated surface in 2D mode, there was an offer in advantages of non-contact optical method in Particle Image Velocimetry for following the developed fluid flow close to the wall without the risk of irreversible damage of the treated surface.



The traditional PIV experimental setup was modified into alignment that enables synchronized measurement of velocity profile over the whole channel and close to the wall in macro scale.[17-21]

For the purpose of this study the measurement were tested on commercial samples of Xylan 1010 and PFA 810 DYKOR at first and in the second step there were treated the brushed stainless steel samples with UltraEver Dry[®] cover and plasmatic treatment with Cr3C2.25 NiCr powder.

Methods

As a part of cooperation with the Masaryk University and CKD Blansko was designed and optimized experimental testing channel of a rectangular shape with (0.08 x 0.08) m cross section for the measurement of the flow close to the wall surface. The whole assembly of the circuit and the installation of actuators (pumps, control valves) with measuring equipment (flow meters, pressure sensors) was set at Technical University of Liberec. To set the precise flow, the circuit was extended with the secondary control bypass. The testing samples were fitted into the cross section and the rest of the channel floor was filled with the strip of material in the same high to avoid the steps affecting the flow. The first task after the assembly of the channel set-up was to determine the flow profile entering the measuring area. To monitor the flow profile in the vicinity of the special surface is required to ensure that the flow is steady and fully developed in laminar region. For this reason the testing chamber was extended with channel adapter. The sufficiently stable flow was found in the distance 1750 mm from the inlet orifice. According to the channel inner diameter was set the Re 1030, which corresponds to the flow 5l/min.

The experimental setup

The main deal of this project was to apply the measuring method that enables qualitative description and characterization of the liquid flow that interacts close to the wall with smart surfaces in the context with fully developed laminar flow. There were expected very small changes in the velocity profile so all the contact methods such as Hot-wire anemometry or Prantle probe were excluded. The second condition was not to disrupt the surface. According to the review of characterization near-wall flows there was chosen the noncontact optical method Particle Image Velocimetry as a main measuring technique. This method enables to measure velocity fields in complex and turbulent flows and allows spatial studies of near-wall flows.

The Particle Image Velocimetry (PIV) system here uses the double pulse Nd:YAG laser and two digital CCD camera Neo with a spatial resolution of 5.5 Mpixels; both produced by Dantec Dynamics. As seeding particles was used fluorescent dye Rhodamine B of monodisperse size 10 μ m. The cameras were set in the alignment with optical prism that enabled to observe the same area and using different optical lens system we reached to capture the whole profile velocities and the macro view for the close to wall velocity profile investigation. In every run 200 image pairs were acquired. These images were processed by cross-correlation (interrogation area 64 x 64 pixels, overlap 25%); range validation and vector statistics done by the DynamicStudio software.

The investigation of the surfaces characteristics was completed with the shadowgraphy optical measurement of the contact angle – static and dynamic behavior of the droplet. For the purpose of this measurement we set the upgraded shadowgraphy setup consisted of high speed camera



SpeedSense – DantecDynamics and software PCC2.1. The continuous light source of 1.5kWatt was focused to the path of the drop and placed oppositely to the camera. Using this setup with very small exposure time and the aperture number 4 we obtain quality image with high contrast. Images were received and digitized by a CCD high speed camera. The whole system, including storage of images, was controlled by a personal computer. The sample rate was set 5000 fps, the exposure time of the CCD-camera was $1.02\mu\text{s}$ with image resolution (1280x800)px. During the measurement we used the pre trigger of 1sec time and the measurement was synchronized by the photocell. The data obtained from the measurement were mathematically processed and analyzed. The impinging drop method give us information about wettability of the substrate that can be also described with the static contact angle and the second condition that can influence the droplet behavior is the surface average roughness. Using this method we can study the process of droplet kinetic energy dissipation by viscous effects and surface energy that is demonstrated by dynamic behavior.

This testing of surfaces before the examination with PIV method in the testing channel became of extreme importance as we realized losses in the superhydrophobicity during the measurement. In the testing channel each sample was exposed to the constant flow for at least 20minutes till the experimental setup was finished and during the measurement. The commercial testing usually includes the CA or SA behavior and also the results of these methods are mostly unrepeatable till the surface is completely dry again. In our testing chamber the sample underwent the action of the liquid over the whole area. The measurement of CA and SA revealed the decrease of 10% from the initial value after each measurement in the testing chamber. These changes of surfaces property also took shape in the velocity profile.

Discussion / Interpretation of Results

For the first test flow measurement were selected boards from usual materials such as: glass, Stainless steel – brushed (CA from 92° to 72°) and the tetrafluoroethylene (PTFE). The different CA of Stainless steel was explained via the oil layer due the conservation of the surface and to avoid the effect of humidity. During the testing the oil layer was removed and we measured the rough brushed surface with final value of CA 72° . The PTFE belongs to the one of the first and so far still used substances of very low surface energy (20 mN m^{-1}), good thermal stability and excellent mechanical properties. Here we tested two commercial samples: XYLAN 1010 – that is mechanical resistant and PFA 810 DYKOR that shows less surface roughness and is softer. The prescribed surface tension of these materials should be round 100° . The stainless steel sheet treated with electrochemical method and covered with Cr3C2.25 NiCr stabilized under very high temperature shown CA 125° . As the referring material with well know contact angle velocity flow profile was chosen pure glass (CA 28°).

Figure 1 shows the velocity profiles over the whole width of the cross section. The maximal velocities of the flow by various boards (glass, stainless steel, XYLAN 1010 and PFA 810 DYKOR and surface of treated stainless steel) do not differ. Nevertheless the position of maximal velocity peaks differs according to the surface. According to the degree of hydrophobicity there is seen the shift in the slope of the ramp of the profile anyway the surface below the curve is of the same value. This characteristic is also demonstrated in the decrease of the maximum velocity and more flattened shape of the velocity in the middle section of the whole velocity profile compare to the initial laminar shape velocity profile. In the case of pure glass – with very low CA, there is visible gap and the profile



is developing at the distance 8mm far from the wall. In this case there was developed symmetric laminar velocity profile with higher maximum velocity. Figure 2 shows the results of each measurement as the scalar and vector map. The accurate position of the velocity profile was in the middle of the picture. The zero mark on y axis is fixed to surface and the maps show the changes in fluid behavior according to the stratification of the flow layers. The top part of the map and velocity profiles is influenced with the physical properties of the channel wall – in our case the plexiglass. As the chamber is not axis symmetric the fluid flow behavior is affected by both sides but we presuppose the laminar flow in the channel without the presents of any sample. During this measurement the dynamic range of the PIV measurement was set to cover the maximum speed of liquid in the testing chamber for this reason the velocity closer to the wall, means the distance from 0 to 10mm far from the surface, cannot be properly calculated due the slowing down and changes in dynamic range. From this condition emerged the need of the second synchronized measurement with different dynamic range setting that enables cover the very slow velocity and the braking of the fluid flow close to the wall.

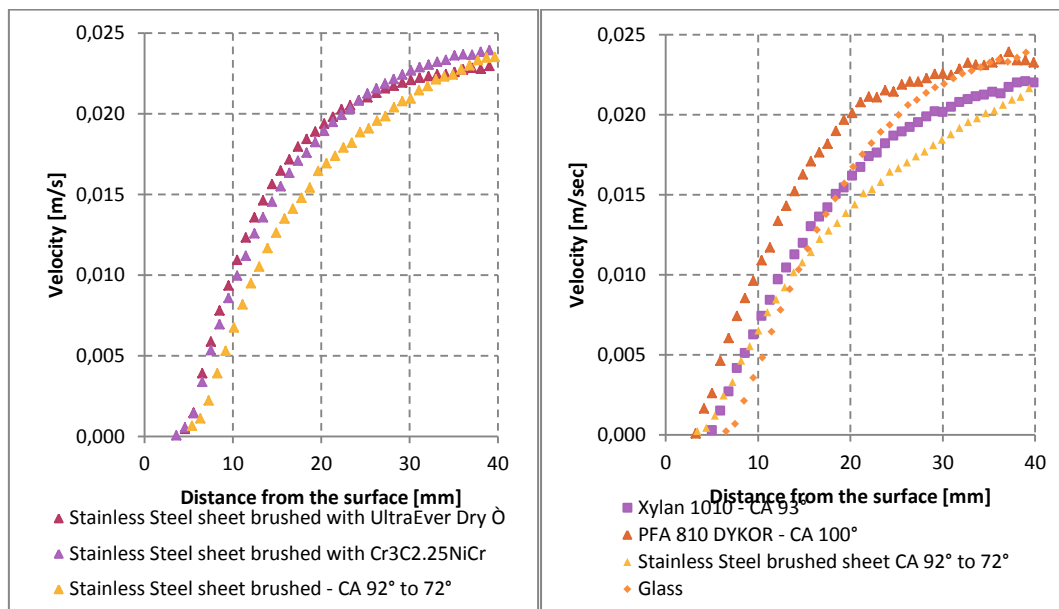


Figure 1 Velocity profiles for the laminar flow 5l/min, Re 1030, the chart represent the development of the flow close to the surface and up to the middle of the channel.

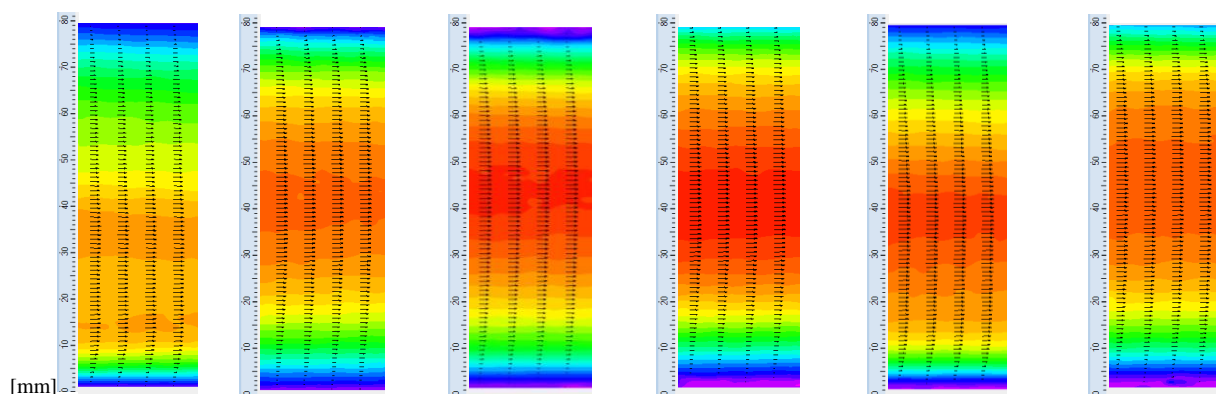




Figure 2 Scalar and vector maps for the laminar flow 5l/min, Re 1030, the chart represent the development of the flow close to the surface and up to the middle of the channel.

Figure 3 shows the results of the measurement taken with the camera that run in the macro range and set for the dynamic range that cover the fluid velocity in the near-wall section. The scaled velocity profile in the area between zero (surface) and 20mm far from the surface demonstrates the relation between the surface hydrophobicity and the slope of profile curve. There is expected the significant change for the ultrahydrophobic surfaces with $CA > 150^\circ$.

With the optimize measurement setup for the dynamic range of slower near-wall velocities the velocity profiles reveal the characteristics of the flow and refine the maximum velocities. This explains the velocity shift and differences between the measurements on the whole profile setup.

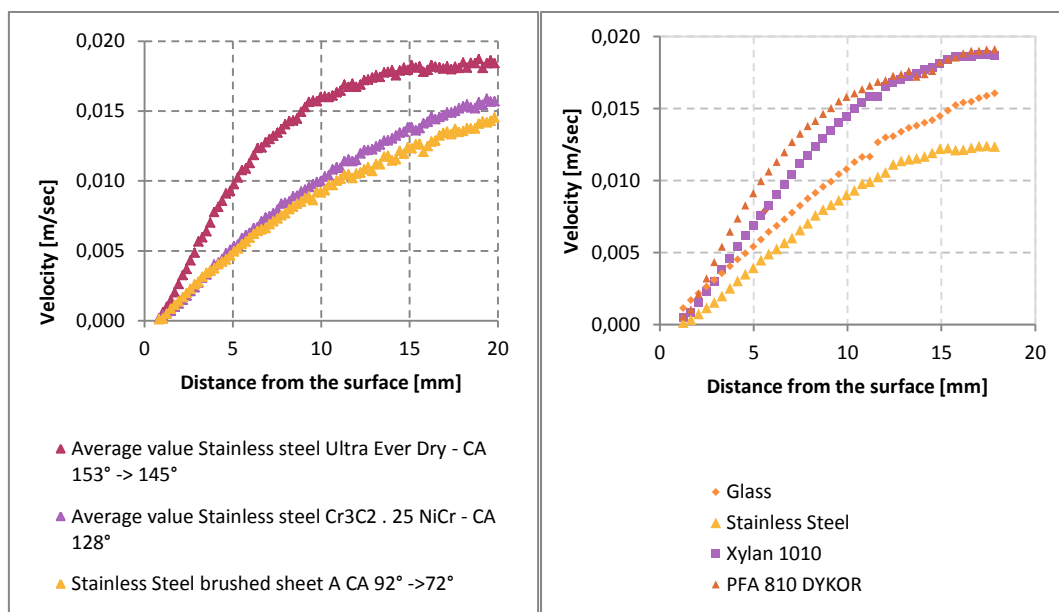


Figure 3 Velocity profiles for the laminar flow 5l/min, Re 1030, the chart represent the development of the near-wall flow close to the surface acquired with measurement optimized to the dynamical range of slow flow.

Figure 4 shows the scalar and vector maps that describes and quantified the fluid near-wall flow behavior. These results represent the significant changes in stratification of near-flows that reflects in the more distant flow structures. Anyway the measurement was optimized to the dynamic range the very near-wall velocity measurement is influenced by the behavior of particles itself and in the interaction of the ultrahydrophobic surface properties here come up the interaction between the air foil structure that has to be count in the interpretation of the final results in sense of the profile shift. With this near-wall measurement we also reached the technical limit of the laser system and the synchronizing unit. This can be partly solved with the external synchronization.



The second area of improvement is in the numerical processing of acquired dataset. With this problem deals Y. Zhu [17] and offers novel solving algorithm specially suggested for solving near-wall regions.

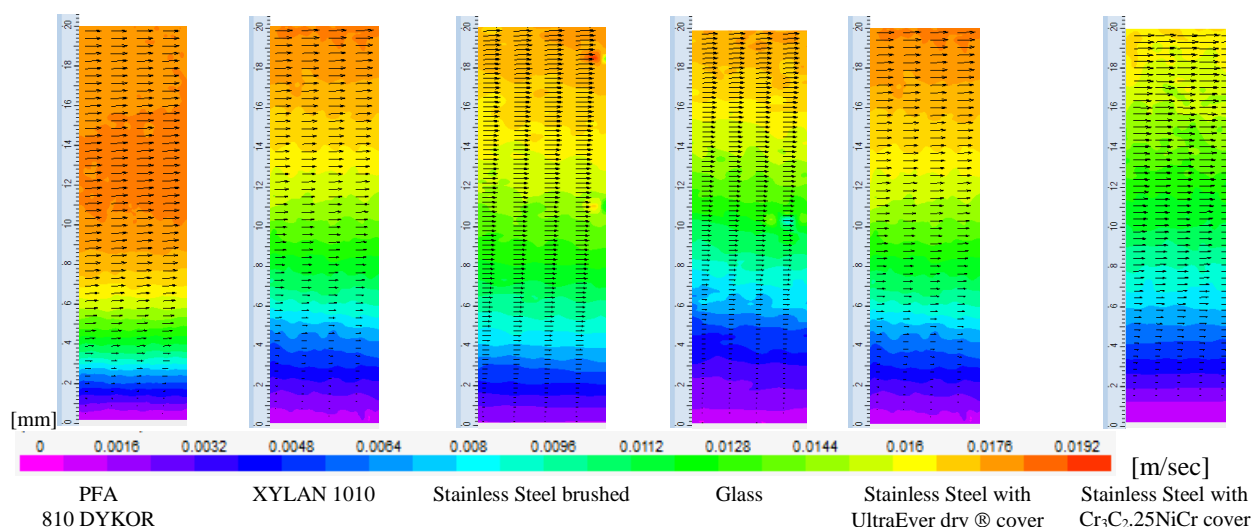


Figure 4 Scalar and vector maps for the laminar flow 5l/min, $Re\ 1030$, the chart represent the development of the flow close to the surface measured with macro scaling.

As it was mention above the samples were tested using Shadowgraphy method and pendant drop method on CA and SA. The images were analyzed with our software that is designed on the contact angle analyses. This noncommercial software does not approximate the drop with the circle but analyze the curve from the contact point and space the tangent following the whole droplet profile. This method provides more precise result in comparison with other methods. The measurement of CA was set with distilled water and the pure glass CA was 28° , the electrochemically treated surface of Stainless Steel was 84° . The XYLAN 1010 with rough surface fulfils the prescription of the manufacturer and we measured the contact angle of 100° and for PFA 810 DYKOR with soft and smooth surface 93° . The highest CA from our samples reached the Stainless Steel treated with UltraEver Dry® coating 153° but after one run of measurement the CA decreased on value 148° and was stabilized on value 145° . The steel plasmatic treated and covered with $Cr_3C_2.25\ NiCr$ powder stabilized with heat shown stable CA of 128° .

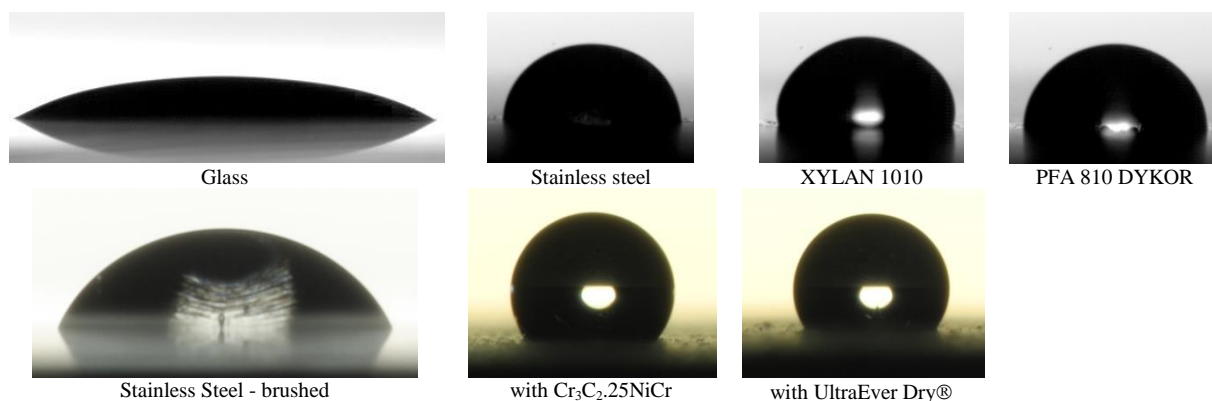


Figure 5 The sessile water drop on the investigated surfaces.

Conclusion

The measurement brought results of the close wall flow measurement in the context of whole profile measurement over the testing channel width. The both measurement were realized using PIV technique.

For better understanding of this effect the macro scale study close to the boards' surfaces was made. Here we deal with commercial materials XYLAN 1010 and PFA 810 DYKOR, brushed stainless steel, glass, the stainless steel sheet covered with UltraEver Dry[®] nanolayer and stainless steel with plasma treatment and covered with Cr3C2.25 NiCr powder. The surface modification causes the change of velocity profile in the way that velocity increases with the distance from the board faster. This could be affected by the boundary layer width. It is presumed, according to the PIV measurement's findings, that here the boundary layer is turbulent. The edge of the turbulent boundary layer is a spatially and temporally strongly fluctuating surface. It seems that hydrophobic surfaces change the turbulence of boundary layer.

During the measurement of near-wall flow we reached the technical limits of the PIV method and the further improvement in following very slow flows via external synchronization units can move this kind of investigation. The measurement directly related to the surface properties such as CA gave us novel information that the static tradition method can be completed by the dynamic one and the results are consistent.

References

- [1] F. Pochyly, et. al, *International Journal of Fluid Machinery and Systems* 3(4), 386 – 394 (2010).
- [2] C.A.E. Hamlett, et. al, *European Journal of Soil Science* 64, 324–333 (2013).
- [3] C.-H. Xue, S.-T. Jia, J. Zhang, and J.-Z. Ma, *Science and Technology of Advanced Materials* 11(3), 033002 (2010).
- [4] P. Hao, C. Lv, Z. Yao, and F. He, *Europhysics Letters* 90(6), 66003 (2010).
- [5] A. Mongruel, *Journal of Physics: Conference Series* 392, 012011 (2012).
- [6] H.-B. Hu, P. Du, S.-H. Huang, and Y. Wang, *Chinese Physics B* 22(7), 074703 (2013).
- [7] N. Yurchenko, *Physica Scripta T132*, 014011 (2008).
- [8] M. Leschziner, H. Choi, and K. Choi, *Philosophical Transactions of the Royal Society A: Mathematical, Physical and Engineering Sciences* 369(1940), 13491351 (2011).
- [9] A. Nakayamaa, H. Nodab, K. Maedac, *Fluid Dynamics Research* 35, 299–321 (2004).
- [10] G. Kawahara, *Fluid Dynamics Research* 41(6), 064001 (2009).
- [11] S.-Q. Yang, *Fluid Dynamics Research* 36, 121–136 (2005).
- [12] E. Gnanamanickam, B. Nottebrock, S. Große, J. Sullivan, and W. Schröder, *Measurement Science and Technology* 24(12), 124002 (2013).
- [13] B. C. Khoo, Y. T. Chew, C. J. Teo and C. P. Lim, *Meas. Sci. Technol.* 10, 152–169 (1999).
- [14] B. Nottebrock, S. Große, and W. Schröder, *Journal of Physics: Condensed Matter* 23(18), 184121 (2011).
- [15] D. H. Ferriss, *Aeronautical research council* 831 (1965).
- [16] J. Foucaut, S. Coudert, and M. Stanislas, *Measurement Science and Technology* 20(7), 074004 (2009).
- [17] Y. Zhu, N. Yuan, C. Zhang, C Lee, *Measurement Science and Technology* 24, 125302 (2013).



[18] C. Kähler, U. Scholz, and J. Ortmanns, *Experiments in Fluids* (2006).

[19] E. Aljallis, et.al, *Physics of fluids* 25, 025103 (2013).



B. Measurement of the air layer in the liquid boundary layer near the hydrophobic surface.

C. Evaluation of measurement, correlation with the mathematical model and computational modeling.

Introduction

The measurement method that gives us complex information about the flow is offered as on macro scale i.e. Particle Image Velocimetry (PIV). Because here we dealing with micro and nano scales the tradition PIV fitted with magnifying lens system constitutes sufficient background for the measurement setup. [1-6]

Micro-channel setup

The fabrication of the micro-channel is one of the areas of the microfluidic research. Nowadays there exists a traditional method based on the negative resist using lithography, plasmatic etching, or streaking.

Here in this study we have tested a couple of recommended method but the only of the combination of the rapid prototyping and plasmatic bondage was successful.

The rectangular micro-channel was designed with the depth d 3mm and width 5mm of the final length 100mm. The construction is seen on the figure 1.

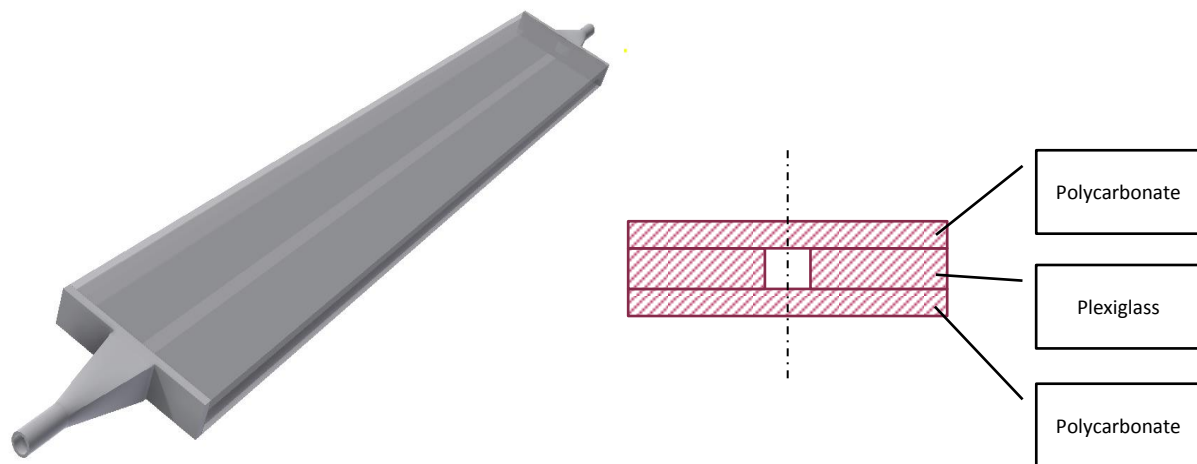


Figure 1 construction of the segment for the measurement of the liquid boundary layer

The inner cavity is developed after plasmatic bonding of all segments and is joined to the recirculation via connectors that were manufactured on 3D printer. This mounts fit with ordinary Luer-lock system. The fluid flow was generated with two separate laboratory syringe pump or the peristaltic pump. Here we used distilled water that was driven through the micro-channel. The mounts are about to be set with the pressure sensors for the monitoring of the pressure loses in the whole chamber due the changes of the friction coefficient.

Here we set the flow velocity according to the knowledge of the laminar flow and the Reynolds number range in micro fluidic. Due the friction factor the transition area in Re starts at 1000.

$$D = \frac{4A}{P} = \frac{2(W_a+W_b)d}{W_a+2b+W_b} \tag{1}$$

$$Re = \frac{\bar{u}D}{\nu} \tag{2}$$

, where u is the mean channel velocity, D is the hydraulic parameter and ν is the kinematic viscosity of water ($1,004 \cdot 10^{-6}$ for 20°C)

The hydraulic parameter for the micro-channel is 3.75mm. The Reynolds number in mini-channels with similar hydraulic parameter for laminar flow was experimentally set as 550. Above this edge the flow shows irregular directions and for Re round 1000 is set to be turbulent. The transient area was established $240 < Re < 1000$. [2]

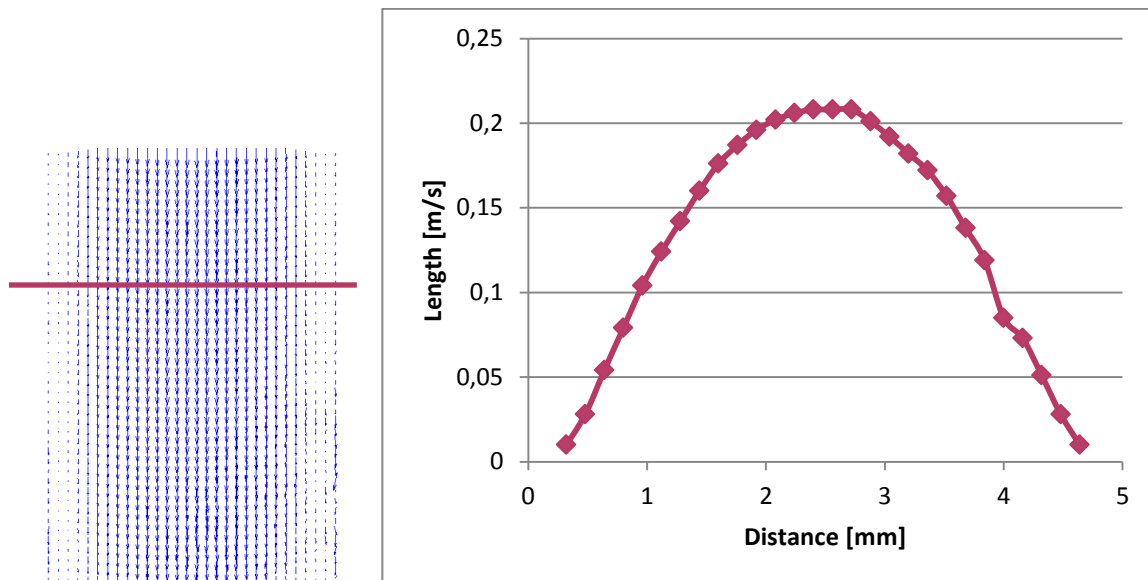


Figure 2 construction of the segment for the measurement of the liquid boundary layer

Micro-PIV measurement setup

The micro-PIV measurement setup is based on the magnifying optical system. He we used Leica DM IL inverted laboratory microscope set with standard objective, for our measurement we used 10x.

The micro-PIV consists of NewWave Gemini Nd:YAG pulsed laser of energy in each pulse 120mJ. The duration of one pulse was 10ns and the wavelength of the laser 532nm.

The images were captured using Neo CMOS camera with 5,5MPixel resolution and pixel size 6,5µm, Pixel well depth (typical) 30,000e- and cooling system for noise reduction.

The laser light and the camera were synchronized via timer box.



In standard PIV method the depth of field is influence of the distance from the measured object, selected lens system and f number. In micro-PIV the depth of field depends on the microscope objective and its parameters, refractive index n of the fluid in the microfluidic channel, λ the wavelength of used light. The other parameters that relate to the micro lens system: NA – numerical aperture of objective lens, M – total magnification of the system. The last parameter influencing the depth of field is the spacing between pixels in CCD chip of the camera e.

$$\delta = \frac{n\lambda}{NA^2} + \frac{n.e}{NA.M} \quad (3)$$

For our measurement setup according this quotation the depth of field is $4\mu\text{m}$. This factor has to be taken into account while choosing the seeding media and also focusing over the channel depth.

There exist special rules for seeding medium in micro-PIV. The first condition is the particle visibility. The quality of captured images strongly depends on the contrast of the particles against background.

There are visible only those particles that merge the depth of field and are illuminated. The background reflects the scattered light from the particles. This disadvantage of the lighting is partly reduced using fluorescent technique. Here we used the Rhodamine B particles that emit light on 570nm . The background noise is mostly caused by unfocused moving particles and this is difficult to remove.

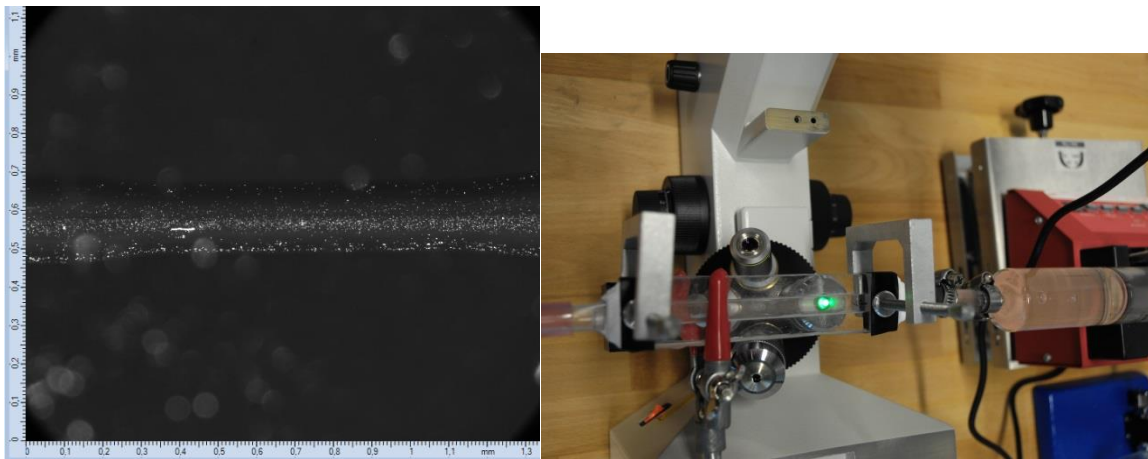


Figure 3 the structure in the microscope view illuminated by the laser light, the fluid flow seeded with fluorescent particles

The next parameter of the seeding medium is its size. There exists the limit when the size of particles is small and the collective effect of collisions and fluid molecules is unbalanced. [1] This behaviour is called as Brownian motion. The suitable size of particles can be chosen considering to flow dynamics. Here we evaluate the ability of single particle follow the flow. This parameter is set with the response time τ .

$$\tau = \frac{d^2\rho}{18\mu} \quad (4)$$

, where d is the particle diameter, ρ the particle density and μ the dynamic viscosity of fluid.

According to the quotation (4) we seeded the fluid with $5\mu\text{m}$ PS Rhodamine B labelled particles. The response time of the particle is 10^{-5}s . According to the fluid speed (units' mm/s) the response time is small enough for particles to follow the flow sufficiently.

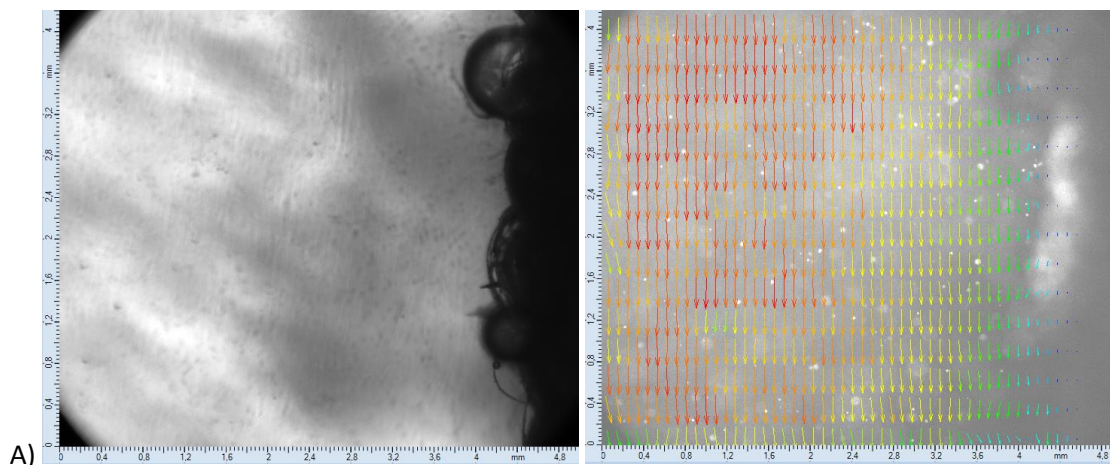
The last error that should be mentioned here in the relation to the seeding is the particle position error. This error corresponds with the Brownian motion, displacement and the time of exposure time of the laser light. This error can be neglected when the Brownian motion is small according to the size of particle.

The captured images were pre-processed with masking function. The images were processed with adaptive correlation. This kind of correlation is the approach in cross-correlation. This method is optimized to the local displacements. The sizes of interrogation areas are locally adjusted to the maximal velocity of the fluid flow. This method is crucial to micro fluidics because it can describe big local velocity changes in a small spatial scale, where is impossible to adapt the dynamic range via time between pulses. Here we used the adaptive correlation algorithm setup with minimum size of interrogation area (32x32) pixel and maximum size (64x64) pixel in 8 iteration steps.

The calculated raw vector maps were also validated while adaptive correlated. The validated vector maps were statistically processed and the dataset were interpreted via Tecplot software.

Results and discussion

In the first part of the experimental study, the micro channel was tested on the laminar flow profile. The figure 4 shows the results of the measurement close to irregular surface, and the regular pattern.



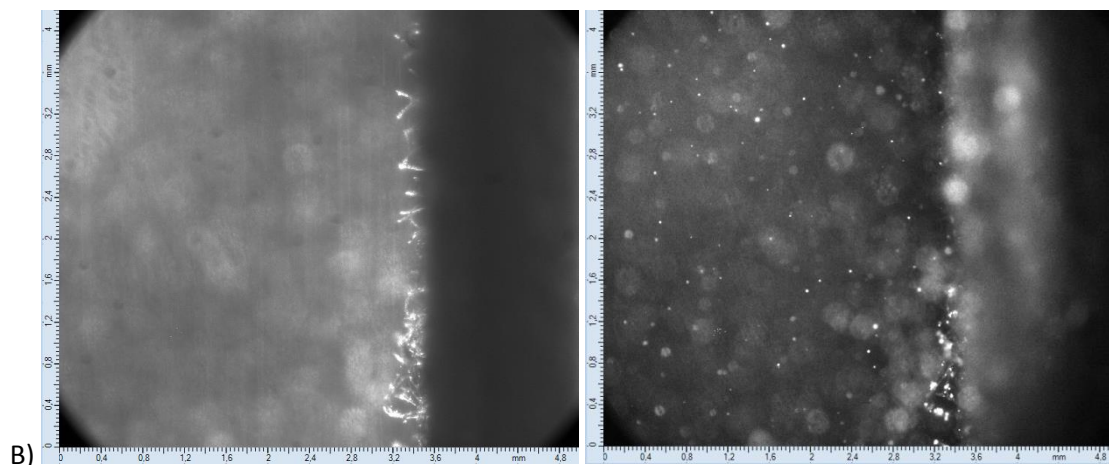


Figure 4 A) the textile sample in the micro – channel and the calculation of the velocity profile close to the irregular surface and B) with the regular pattern.



Figure 5 the bubbles on the structures of scales as the example of the situation on the patterned surfaces with the contact angle 120° .

Conclusions

This study presented the results of micro-PIV measurement in the micro-channel rectangular cross-section. The next steps in solving this problem are focused on “the close to wall study” that could uncover the fluctuation behind the structure in the flow direction. The micro-PIV technique is suitable for study of the interactions in the micro structures and cavities with optical access.

For the purpose of initial measurement the micro-channel was fitted with regular and irregular textile structure with the proved contact angle of 120° . As the liquid flow was kept on the $Re\ 550$ to ensure the laminar profile; on the surface raised bubbles. Due the low flow rates this unique bubble had not created a continuous layer. This was the main reason why we could not use the tomographic system here. Anyway the size of the single bubble is measurable and it is varying between $40\mu\text{m}$ to $200\mu\text{m}$.

References

- [1] M. Raffel, et. Al., *Particle Image Velocimetry - A Practical Guide*, Springer Berlin Heidelberg, 2007, ISBN 978-3-540-72307-3
- [2] S.-S. Hsieh, et. Al., *Journal of Micromechanics and Microengineering*, 14, 4, 2004.
- [3] P.-F. Hao, et. Al., *Journal of Micromechanics and Microengineering*, 16,7, 2006.
- [4] P.-F. Hao, et. Al., *Journal of Micromechanics and Microengineering*, 15, 6, 2005.
- [5] S.-S. Hsieh and Y.-C. Huang, *Journal of Micromechanics and Microengineering*, 18, 6, 2008.
- [6] M. Mielnik and L. SaeTRAN, *Experiments in Fluids*, 41, 2, 2006.

The publications dedicated to the foundation

D., Jasikova, L. Nemcova, V. Kopecky, The method for Study of Smart Surfaces Using PIV Technique, AIP Conference Proceedings, 1608, pp. 80-87, 2014

D. Jasikova, M. Kotek, The estimation of dynamic contact angle of ultra-hydrophobic surfaces using inclined surface and impinging droplet methods, EPJ Web of Conferences, 67, 2014

D. Jasikova, M. Kotek, V. Kopecky, The feasible study of the water flow in the micro channel with the Y-junction and narrow structure for various flow rates in Proceedings of Experimental Fluid Mechanics 2014, Cesky Krumlov, pp. 236-241, 2014

Recommendations

Plan for the year 2015:

- Study of the influence of adhesion coefficient on the formation of vortex structures depending on the Coand effect using the computational modelling
- Study of the influence of adhesion coefficient on the cavitation formation and the cavitation zone width.
- Validation of a mathematical model of the new hydrophobic surface boundary condition

